

Effect of partial atomic charges on the calculated free energy of solvation of poly(vinyl alcohol) in selected solvents

Abolfazl Noorjahan · Phillip Choi

Received: 18 September 2014 / Accepted: 30 November 2014
© Springer-Verlag Berlin Heidelberg 2015

Abstract It is well-known that properties of poly(vinyl alcohol) (PVA) in the pure and solution states depend largely on the hydrogen bonding networks formed. In the context of molecular simulation, such networks are handled through the Coulombic interactions. Therefore, a good set of partial atom charges (PACs) for simulations involving PVA is highly desirable. In this work, we calculated the PACs for PVA using a few commonly used population analysis schemes with a hope to identify an accurate set of PACs for PVA monomers. To evaluate the quality of the calculated parameters, we have benchmarked their predictions for free energy of solvation (FES) in selected solvents by molecular dynamics simulations against the *ab initio* calculated values. Selected solvents were water, ethanol and benzene as they covered a range of size and polarity. Also, PVA with different tacticities were used to capture their effect on the calculated FESs. Based on our results, neither PACs nor FESs are affected by the chain tacticity. While PACs predicted by the Merz-Singh-Kollman scheme were close to original values in the OPLS-AA force field in way that no significant difference in properties of pure PVA was observed, free energy of solvation calculated using such PACs showed greater agreement with *ab initio* calculated values than those calculated by OPLS-AA (and all other schemes used in this work) in all three solvents considered.

Keywords Poly(vinyl alcohol) · Molecular dynamics · OPLS-AA · Partial atomic charge distribution · Free energy of solvation

Introduction

Poly(vinyl alcohol) (PVA) and its blends with other polymers and composites filled with fibers are found in numerous technological applications [1–5]. To process the materials, solvent is usually needed. Water is the only known practical solvent for PVA but it only works over a limited range of temperatures. Solvent mixtures containing a significant amount of water are also used [6]. Despite the presence of the hydroxyl moiety, both vinyl alcohols (e.g., ethanol) and carboxylic acids (e.g., acetic acid), are known to be immiscible with PVA [7]. This implies that identifying new solvents for PVA based on the idea of matching chemical functional groups not as fruitful as one might expect. Nevertheless, being able to find solvents other than water is desirable for some applications of PVA in which PVA involves in reactions to form water-insoluble derivatives [6].

Owing to the cost and time consuming nature of experimental procedures, molecular dynamics (MD) simulation seems to be a cost effective, viable alternative to design solvents of interest [8–15]. It is well-known that accuracy of the MD simulation is mostly dictated by the quality of the force field used. A well parameterized force field can accurately reproduce experimental measurements in a much efficient fashion. Needless to say, before doing any extensive simulations on any polymer/solvent sets, checking the accuracy of the force field adopted is an essential step.

A. Noorjahan · P. Choi (✉)
Department of Chemical and Materials Engineering,
University of Alberta, Edmonton T6G 2V4, Canada
e-mail: phillip.choi@ualberta.ca

Most of the known properties of PVA are attributed to its strong hydrogen bonding network [2–4, 15–30]. Obviously, introducing solvent molecules into the polymeric matrix will disturb such network. Interactions between PVA and solvent molecules are affected by both the size of the solvent molecules (breaking hydrogen bonds) and the ability of the hydrogen bonding network to accommodate the solvent molecules. For example, in the case of water, its small size and strong hydrogen bonding capability are both in favor of mixing. Keeping this in mind, an accurate prediction of the hydrogen bonding interactions in any PVA/solvent systems is crucial.

In the context of MD, hydrogen bonds are usually handled through the Coulombic interaction. As a result, partial atomic charges (PACs) become the tuning parameters. To have an accurate prediction of the hydrogen bonding interaction, a set of well-tuned PACs are required. The process of tuning PACs in a force field is not a trivial task even for small molecules [31–33]. A common practice for developing a force field for polymers is to optimize the PACs to reproduce key properties of small molecule analogs [31] and then to extend the results to the corresponding polymeric systems. However, there is no guarantee that the optimized PACs based upon the small molecule analogs are able to reproduce the properties of the polymers where conformation and tacticity also play a major role [34]. Accordingly, in this work, we replaced the empirical optimization of PACs by using quantum mechanically derived electrostatic potentials fitted to selected point charge models [33].

There exist several conventional methods that can be used to derive PACs directly using the electron density obtained from ab initio calculations [35]. To select the best PAC set for PVA, we have benchmarked the free energy of solvation (FES) for PVA oligomers in selected solvents calculated from MD simulation using PAC sets obtained from various point charge models against the ab initio calculated values. To capture the effect of tacticity, we have repeated the calculations for long enough PVA oligomers with different tacticities (atactic, isotactic and syndiotactic). Solvents used in this study were water, ethanol and benzene. They were chosen as they have different sizes and hydrogen bonding capabilities. In this work, we retrieved all bonded and non-bonded parameters except PACs from the original OPLS-AA force field. As in our previous work [36] we showed that the OPLS-AA force field can reproduce properties of PVA in its pure state reasonably well. Effects of chain conformation and tacticity [34] on the PACs were studied in this work. Here, we identified a set of PACs for PVA which can reasonably predict the interactions between PVA and the selected solvents. Another major contribution of this work is the identification of a point charge model for the

calculation PACs compatible with the OPLS-AA force field for similar systems when proper values are missing.

PVA oligomers

All oligomers used in this study had 10 repeating units capped with two methyl groups. This size was selected as a compromise between the computation cost of ab initio calculations and capturing the tacticity effect without any significant end effects. All calculations in this study repeated for isotactic, syndiotactic and atactic PVA (with 50 % chance of chiral center inversion). Similar to previously reported work [37], all monomer connectivities are head-to-tail.

To create the required structures for calculations, a chain with the tacticity of interest was created using the Amorphous Builder module in Materials Studio 5.01 [38] at very low density (vacuum). In the next step, this chain went through a geometry optimization using the original OPLS-AA parameters in GROMACS to remove close contacts, if any. This was followed by an equilibration MD simulation in vacuum at 400 K. Finally, a short, 5 ns, simulation at 400 K in vacuum was performed on the chain and snapshots were saved every 100 ps (a total of 50 different snapshots saved for each chain). All ab initio and MD calculations were repeated for every snapshot created here to capture the effect of conformational changes on the calculated properties as per the method of [39, 40]. For the calculation of FES at the ab initio level, an implicit solvent model (see the section on the Calculation of FES) was used. At the MD level, each oligomer was mixed with 1000, 400 and 231 molecules of water, ethanol and benzene, respectively, in a three-dimensional periodic box. These numbers were determined by trial and error to keep number of solvent molecules and the system size effect on the calculated FES at the minimum simultaneously.

ab initio calculation

Calculation of PACs

For all ab initio calculations, we used the Gaussian09 package [41] and the level of theory used was UB3LYP/6-31G* [42]. It was used previously in the calculation of partial atomic charges used in the AMBER force field [32, 33] but is different from that (RHF/6-31G*) used in the development of the original OPLS-AA force field [31]. Having the basis set (energy) converged for a molecular system, a few selected population analysis methods were used to calculate the PACs. In this study, we used the Mulliken

Population Analysis (MPA) [43], Natural Population Analysis (NPA) [44], Merz-Singh-Kollman (MSK) [45, 46], Atoms In Molecules (AIM) [47] and Hirshfeld [48–51] methods. All aforementioned methods are incorporated in the Gaussian09 package except the AIM method that we used the “Bader Charge Analysis” code [32] for the post processing of the data. It is worth mentioning that to obtain accurate results, cube files generated by Gaussian09 were exported with fine meshing. In addition, as other researchers suggested [35], we used 2,000 points for each atom when the MSK scheme was used. The following summarizes the procedure for the calculation of PACs.

- First, PACs were calculated for all snapshots created by the 5 ns MD simulations in vacuum. The level of theory for this calculations was UB3LYP/6-31G*. Note that it has been reported that PACs calculated using UB3LYP/6-31G* are very close to the results of high quality ab initio calculations [35]. These values will be used to discern the effect of geometry optimization.
- Then, using the same level of theory, all snapshots have been geometry optimized in vacuum and PACs were calculated for these optimized structures.
- Finally, each oligomer (snapshot) was solvated in implicit solvent (either water, ethanol or benzene) using the Polarizable Continuum Model using the integral equation formalism variant (IEFPCM) [52] method. Then, using converged basis sets in implicit solvent environment, PACs were calculated again.

The SCF convergence criteria were set to 10^{-n} for the root mean square changes in the elements of the density matrix between two successive cycles with n being 8 for the calculation of SCF energies, gradients and second derivatives. The criteria for the convergence of the geometry optimization were set as follows; 0.00045 and 0.0003 ($E_h a_0^{-1}$) for maximum force and the root mean square of the forces, respectively; 0.0018 and 0.0012 (a_0) for the maximum displacement and the root mean square of displacements, respectively.

Calculation of free energy of solvation

For the calculation of free energy of solvation, the IEF-PCM method available in the Gaussian09 package was used. For the topological model we used the UAKS which has been obtained from united atom topological model applied on radius optimized for the PBE1PBE/6-31G* level of theory. The electrostatic scaling factor was chosen to be 1.2 as suggested by Wen et al. [53]. The free energy of solvation was calculated simply by subtracting the free energy of each oligomer in vacuum from that in the solvated state. Solvents considered for this work were water, ethanol and

benzene. Note that as Wen et al. [53] previously mentioned and our results confirmed, the geometry optimization in the solvated state is not necessary as changes in both geometry and energy are insignificant.

Molecular dynamics simulation

In this work, we used GROMACS 4.5.5 [54–58] for carrying out all MD simulations. We used the OPLS-AA force field [31] to describe the intra and intermolecular interactions of ethanol, benzene and PVA except the PACs of PVA. For water molecules, the TIP4P model developed by Jorgensen et al. [59, 60] and SPC [61] models were used while all bonds were constrained using the SHAKE algorithm [62] unless otherwise stated.

In all simulations, the Berendsen thermostat/barostat [63] with a time constant of 0.2/1 ps were used to control the temperature/pressure of the simulation box. FES at MD level was calculated at 300 K. Given the short length of the oligomers and plasticization effect of the solvent, this temperature was enough to capture essential conformational changes of the oligomers although there is a high chance of missing conformations with high energy barriers [64, 65]. Newton equations of motion were integrated using the leap-frog algorithm [66] with a time step of 2 fs along with a sampling time of 1 ps. The cut-off distance of the non-bonded interactions was set to 1.1 nm and the Particle Mesh Ewald (PME) [67] method was used for handling the long range Coulombic interactions. The long range dispersion energy and pressure corrections were applied to retrieve the correct density values of the systems.

Slow-growth calculation of the free energy of solvation

For the calculation of FES via MD simulation, we have used the slow-growth coupled with the thermodynamic integration method in the GROMACS package. This method requires a simulation during which the Hamiltonian of the system changes slowly from state A, a solvated chain, to that describing the pure solvent, state B. The required modification of the Hamiltonian, H , is realized by making H a function of a coupling parameter λ : $H = H(p, q; \lambda)$ in such a way that $\lambda = 0$ describes state A and $\lambda = 1$ describes state B. It is known that the change in the system, between states A and B, must be so slow that the system remains in equilibrium [68]. Accordingly, the path between states A and B has been split to 201 intermediate states for proper sampling. These steps are related to gradual removing of the Coulombic and vdW interaction of the chain from the Hamiltonian, each of them in 100 steps (for a typical graph of changes in free energy see Appendix B). At each step, we

simulated the system for 1 ns to obtain proper sampling of the conformational changes in the chain. After determining the Hamiltonian, the total free energy change was then calculated by the Multiple Bennett's Acceptance Ratio (MBAR) [69].

Results and discussion

Atomic partial charges

We collected a total of 292,500 PAC data points for all the systems in this study. Readers are referred to the supplementary information for the details of the PACs averaged over all monomers and snapshots. Upon careful analysis such data, several interesting facts emerged and are summarized as follows:

- PACs on the monomers are independent of their positions in the backbone. Therefore, PAC for each atom was averaged over all atoms of the same type in all monomers and over 50 snapshots (i.e., an average over 500 PAC values for each atom). Figure 1 shows the distribution of the PACs for the oxygen atom as calculated using different population analysis methods before the geometry optimization. As one can see, the distribution is rich enough to produce meaningful averages for each method and tacticity of interest.
- Since the snapshots were taken directly from MD simulations, this means that atomic positions were not at the lowest energy state. Figure 2 compares the PACs before

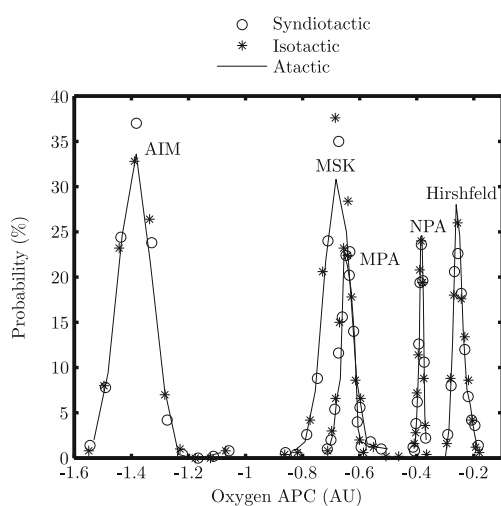


Fig. 1 Probability distribution of the PAC of the oxygen atom in PVA with different tacticities as calculated by different population analysis methods

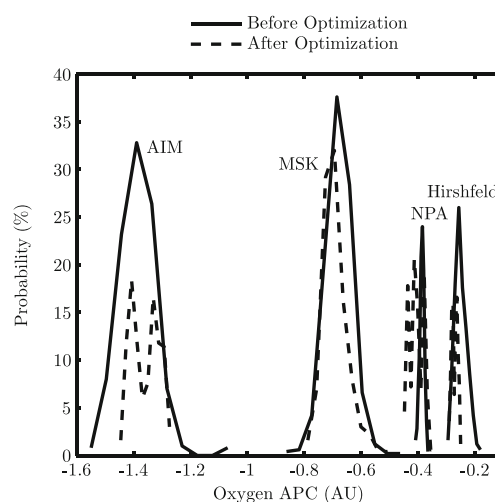


Fig. 2 Probability distribution of the PAC of the oxygen atom in isotactic PVA as calculated with different methods

(Fig. 1) and after geometry optimization. Here, MPA results are not shown for better clarity. As can be seen, all PAC distributions shift slightly. Also, except the MSK method, all other methods show multiple peaks which make determining a unique PAC for each atom more complicated. This observation occurs to other types of atoms too. While MPA results are not sensitive to the geometry optimization, the maximum relative change in the average values of other methods were around 40 % except NPA (500 %). We believe that by a short energy minimization of snapshots at the MD level (keeping the dihedral angles constrained to avoid any change in the chain conformation) the computationally expensive step of ab initio geometry optimization could be bypassed.

- Comparing the PACs for atoms in oligomers with different tacticities revealed that there was no significant differences between calculated PACs. This holds true for all values before and after optimization and even the solvated systems. Based on this result, we can confidently conclude that all the differences between PVA with different tacticities is attributed to their different hydrogen bonding networks and not by any difference in their hydrogen bonding strength.
- In Fig. 3 we have compared the PACs for the oxygen atoms in isotactic PVA in vacuum and in three different solvents as calculated by the MSK method. As it has been reported before [53], our results indicate that there is a minor shift in the PACs in solvents compared to those calculated in the vacuum (the degree of shift is correlated with the polarity of the solvent). Likewise, the same trend was observed for other calculated PACs

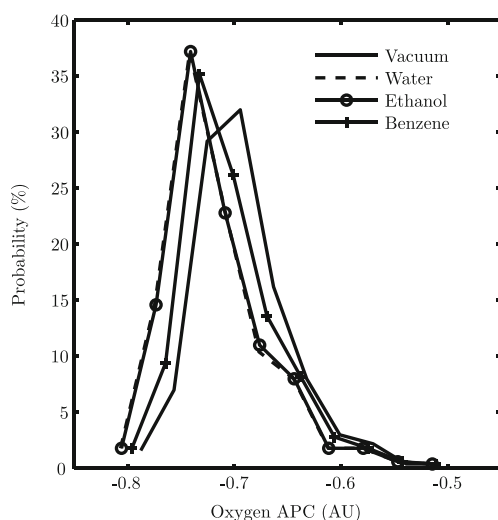


Fig. 3 Probability distribution of the PAC of the oxygen atom in solvated isotactic PVA as calculated by the MSK method

(for detail of the deviations from PACs of optimized structures in vacuum, see the Appendix A). While the sensitivity of PACs from all methods are around 10 % (relatively), the AIM results showed 125 % change respect to optimized values in vacuum. But as environment dependent parameters are not practical for MD simulations and average values are not that different, in this work we used the optimized PACs and ignored the solvent effect.

Based on the above discussion, we selected the PACs calculated for optimized structures in vacuum as representative of each method. Since differences between PACs of different tacticities are negligible, we considered the same PAC set for all stereoisomers where PACs were averaged over all three tacticities. Table 1 shows the final partial charges for each method which were used in the MD simulations. In agreement with previous studies [35], our results show that predictions by the AIM method for the oxygen atom in the hydroxyl group are exaggerated. On the other hand, predictions by the MSK method is moderately damped while the NPA's predictions lies in between of the other two methods. The interesting fact here is how the PACs of the OH group calculated via the MPA and MSK methods are close to those of the original OPLS-AA force field. However, the PACs of both carbon atoms in the PVA monomer calculated from the MSK method are significantly different from the original OPLS-AA force field.

As mentioned before, properties of PVA are mostly dictated by its hydrogen bonding network (or the Coulombic interactions). So, any change in the PACs of the PVA can cause drastic changes in the PVA's properties. Accordingly,

Table 1 PACs of PVA calculated using different population analysis methods

Atom	OPLS-AA	MPA	NPA	MSK	AIM	Hirshfeld
H ^a	0.06	0.149	0.029	0.081	0.019	0.039
H ^a	0.06	0.149	0.029	0.081	0.019	0.039
H ^a	0.06	0.149	0.029	0.081	0.019	0.039
C ^a	-0.18	-0.447	-0.087	-0.243	-0.057	-0.117
H ^b	0.06	0.14	0.027	0.116	0.02	0.042
C1	-0.12	-0.296	-0.063	-0.418	-0.008	-0.054
H ^b	0.06	0.144	0.027	0.109	0.021	0.042
C2 ^c	0.205	0.132	0.107	0.51	0.726	0.112
H	0.06	0.131	0.017	-0.005	0.012	0.045
O	-0.683	-0.657	-0.271	-0.7	-1.353	-0.408
H ^d	0.418	0.406	0.156	0.388	0.582	0.221
H ^e	0.06	0.149	0.03	0.128	0.024	0.042
H ^e	0.06	0.149	0.03	0.128	0.024	0.042
H ^e	0.06	0.149	0.03	0.128	0.024	0.042
C ^e	-0.18	-0.447	-0.09	-0.384	-0.072	-0.126

Note that after averaging the data small changes (third significant digit) has been made in the values for some atoms to make the sum of the PACs for each monomer zero. For the corresponding standard errors of values reported here, see Table 4 in the Appendix A

^aStarting methyl group-Carbon connected to C1

^bConnected to C1

^cConnected to O

^dConnected to O

^eEnd methyl group-Carbon connected to C2

following the procedure presented in our previous work [36], we calculated the properties of pure PVA looking for effect of PACs. In Fig. 4 densities of isotactic PVA at different temperatures calculated using different sets of PACs are shown. The results confirm that values calculated using the MPA and MSK methods are very close to the OPLS-AA predictions. This is not surprising, as it was reported before that PACs calculated using the MSK method are more successful than other methods [35]. Also note that how over estimation of the PACs of the OH group by AIM method causes a dramatic overestimation of the density. Both NPA and Hirshfeld methods underestimate the PACs of the hydroxyl moiety, thereby the density.

In the formulation of the OPLS-AA force field, the non-bonded interactions between atoms connected by 3 bonds (1-4 interactions) are considered with a fudge factor of 0.5. So any change in the PACs of the back-bone carbon atoms of PVA can change the dihedral angle distribution and therefore, the chain's conformation. In Fig. 5, the dihedral angle distribution for the back-bone carbon atoms of an isotactic PVA chain with 400 monomers is shown. Despite the

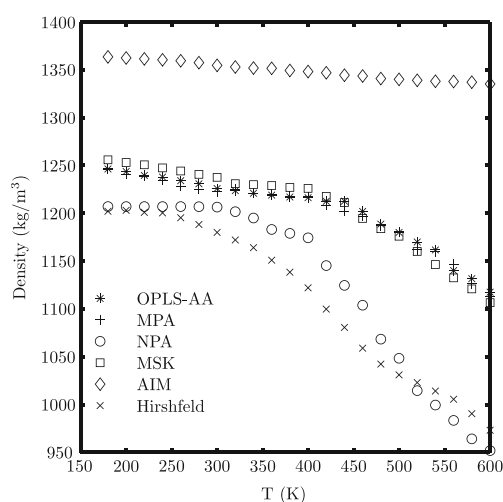


Fig. 4 MD results for density of pure isotactic PVA as a function of temperature calculated using different PAC sets

significant difference in the PACs of carbon atoms calculated by the MSK method with respect to the original OPLS-AA values, the dihedral angle distributions are in good agreement (see the Appendix A for the comparison of the other methods). Note that the minor deviation in the gauche+ can be easily removed by a slight change in the parameters of the Ryckaert-Belleman potential. This trend, close proximity of the MSK results with those of OPLS-AA, holds true for other properties of the PVA (data not shown).

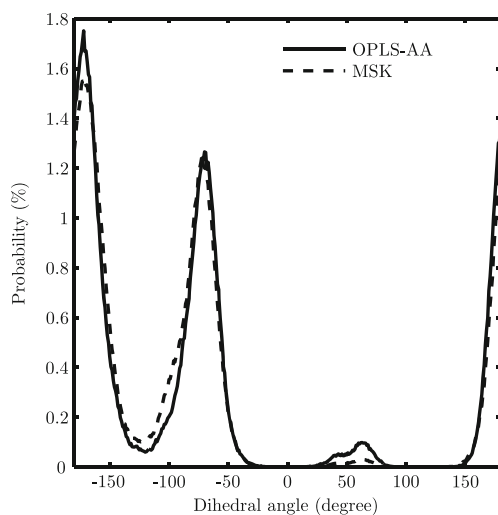


Fig. 5 Comparison of back-bone carbon atoms dihedral angle distribution of an isotactic PVA chain with 400 monomers determined by the original OPLS-AA and MSK PACs. Results were averaged over all possible dihedral angles in a 5 ns MD simulation on a well relaxed chain in a NPT ensemble at 300 K and 1 bar

Free energy of solvation

FES calculated via MD simulations need to be validated by comparing with proper experimental estimations. As no experimental data is available for current hypothetical oligomers, we calculated the FES using accurate ab initio calculations by applying the implicit solvent model [52, 53]. To capture the effect of conformational changes [34], FES was calculated for all snapshots of each tacticities (see the Appendix B). For averaging the FES over all snapshots, data were weighted by a Boltzmann factor [34]. This is necessary as all snapshots were generated at very high temperature (500 K) and the results are about to be compared with values calculated at 300 K in MD simulations. So, averaged values for ab initio calculations shown in the first part of Table 2 were calculated as follows:

$$\begin{aligned} \langle \Delta E_{solvation} \rangle &= \langle E_{sol} \rangle - \langle E_{vac} \rangle \\ &= \frac{\sum_{i=1}^N E_{sol}^i e^{-\frac{E_{sol}^i}{k_B T}}}{\sum_{i=1}^N e^{-\frac{E_{sol}^i}{k_B T}}} - \frac{\sum_{i=1}^N E_{vac}^i e^{-\frac{E_{vac}^i}{k_B T}}}{\sum_{i=1}^N e^{-\frac{E_{vac}^i}{k_B T}}} \end{aligned} \quad (1)$$

where N is the number of snapshots; $\Delta E_{solvation}$ is the FES. E_{sol} and E_{vac} are the absolute ab initio calculated energy of the oligomer in the solvated state and vacuum, respectively; k_B is the Boltzmann constant and T is the absolute temperature here set to 300 K. For the detail of the regular averaged values, readers are referred to the Appendix B. Based on the results, such short PVA oligomers were thermodynamically miscible with all three solvents as the negative value for the FES indicates. While the solvation in solvents with polar groups (water and ethanol) is highly exothermic, the heat released in the case of benzene is significantly lower. Note that the fact that these oligomers are miscible with benzene and ethanol is not in contrast with the fact that PVA macromolecule is not miscible with these solvents. Oligomers used in this study were very short and miscibility of such short oligomers has been reported before in the case of PVA with molecular weights less than 10000 (g/mol^{-1}) [21]. Comparing the FES for oligomers with different tacticities shows that there is no significant difference, another indication that differences between difference stereoisomers of PVA comes from topological differences between their hydrogen bonding network and not conformational differences.

Using the PAC sets developed in previous section we calculated the FES for each oligomer using the MD simulation coupled with the slow-growth method. As each structure evolves during the MD simulation there is no need to repeat this calculation for each snapshot (we repeated a couple of simulations using 5 different initial structures and the results

Table 2 Summary of the calculated FES (kJ mol⁻¹) of PVA oligomers in selected solvents

Method	Tacticity	Solvent		
		Water	Ethanol	Benzene
Ab initio	Ata	-158.3	-149.5	-63.1
	Iso	-155.9	-147.9	-63.9
	Syn	-148.0	-138.3	-56.9
OPLS-AA	Ata	-160.7	-	-
	Iso	-169.3	-169.2	-125.7
	Syn	-159.4	-	-
MPA	Ata	-179.2	-	-
	Iso	-182.2	-168.6	-128.9
	Syn	-180.8	-	-
NPA	Ata	1.1	-	-
	Iso	0.1	-76.0	-89.4
	Syn	0.0	-	-
MSK	Ata	-157.8	-	-
	Iso	-164.5	-156.6	-86.7
	Syn	-154.7	-	-
AIM	Ata	-698.7	-	-
	Iso	-699.6	-526.8	-173.5
	Syn	-740.0	-	-
Hirshfeld	Ata	-34.4	-	-
	Iso	-36.1	-90.1	-101.6
	Syn	-36.6	-	-

The maximum estimated error for MD calculated FES was less than 2 %. For the distribution of the ab initio calculated FES, see the Appendix B

did not show any deviation). Calculated FESs are shown in Table 2. As it was mentioned before in the case of PACs, ab initio calculated FESs exhibited no significant difference between PVA oligomers with different tacticities in water. Accordingly for other solvents, the simulations were limited to isotactic oligomers.

A quick comparison of the MD results with ab initio results reveals that the predictions by NPA, AIM and Hirshfeld PAC sets deviate significantly from the expected values. On the other hand, the predictions by the MPA and original OPLS-AA PAC sets are reasonable for PVA oligomers solvated in water and ethanol. But both PAC sets exhibited

poor prediction for the benzene case. Further, our results suggest that FES calculated by the MSK PAC set gives the best prediction of oligomers solvated in all three solvents with less deviation in the case of benzene. To ensure that water model and the system size do not affect the results, we repeated the calculation using the SPC water model and systems with more solvent molecules. Our results confirm that in all cases, FES deviates no more than 1 % with respect to the values reported here. This insensitivity of the FES to the water model used has been reported previously [70] for drug like molecules.

It is interesting to note that PACs calculated by the MSK scheme are in such great agreement with the OPLS-AA force field and also can predict the solvation energy of PVA in three different solvents even better than using the OPLS-AA PACs. Nevertheless, to check if this holds true as a general rule, such calculations should be repeated for an extended list of solvents and other macromolecules. If successful, the cumbersome task of assigning the PACs to new molecules will be replaced by a series of short and affordable ab initio calculations. In the near future, we will present a comprehensive study on several other polymers and will extend the list of solvents to evaluate the robustness of the approach presented in this work.

Conclusions

To assess the quality of the PACs of PVA used in the original OPLS-AA force field, we collected a rich data set on PACs for short chain PVA oligomers using different conventional population analysis schemes. Our results confirmed that PACs are very sensitive to the initial structures in most of the cases and geometry optimization before PAC calculations is necessary (either at MD or ab initio level). While the sensitivity of the PACs to tacticity of the oligomers was not significant, they showed slightly different values in different solvents. Among all PAC data sets, values of the MSK and MPA schemes were closer to those of the original OPLS-AA force field, and this was reflected in the properties of the pure PVA too. Based on the ab initio results, the FES of PVA oligomers in water and ethanol was lower than those in benzene which is a direct result of hydroxyl groups available in those solvents. While the MD calculated FES using PACs calculated by MPA scheme showed great agreement with values predicted by original OPLS-AA parameters, both showed great deviation for FES of oligomers solvated in benzene. However, use of PACs obtained from the MSK scheme yielded FES values that showed better agreement with ab initio calculated values even in the case of benzene.

Acknowledgments Financial support from the Advanced Foods and Materials Network is gratefully acknowledged. This research has been enabled by the use of WestGrid computing resources, which are funded in part by the Canada Foundation for Innovation, Alberta Innovation and Science, BC Advanced Education, and the participating research institutions. WestGrid equipment is provided by IBM, Hewlett Packard and SGI.

Appendix A: PAC calculation

Table 3 shows the deviation of average PACs calculated in the solvated state using different methods relative to the same PACs calculated in vacuum for optimized structures. As can be seen, the sensitivity of the AIM results to solvent is quite high relative to other methods.

Figure 6 compares the dihedral angle distributions for different PAC sets. As we expected, the quality of results are in accordance with calculated densities.

Table 4 shows the standard deviation of the PACs reported in Table 1.

Table 3 Percentage of relative changes in calculated PACs in the solvated state relative to those of optimized geometries in vacuum

	MPA	NPA	MSK	AIM	Hirshfeld
Water	10	15	39	130	10
Ethanol	9	14	37	123	9
Benzene	10	15	39	130	10

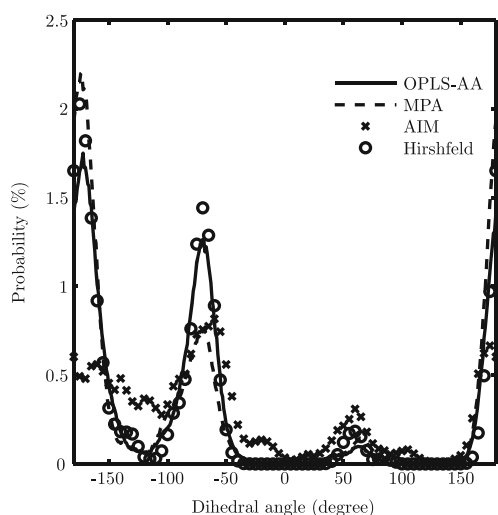


Fig. 6 Comparison of back-bone carbon atoms dihedral angle distribution of an isotactic PVA chain with 400 monomers calculated with different PAC sets. Results were averaged over all possible dihedral angles in a 5 ns simulation on a well relaxed chain in a NPT ensemble at 300 K and 1 bar. Note that the density of the data has been reduced for better resolution

Table 4 Standard error (%) for calculated PACs

Atom	MPA	NPA	MSK	AIM	Hirshfeld
H ^a	0.92	0.33	1.42	1.16	0.37
H ^a	0.94	0.35	1.43	1.24	0.39
H ^a	1.04	0.38	1.50	1.26	0.43
C ^a	1.19	0.15	4.54	1.07	0.13
H ^b	1.46	0.50	3.60	1.56	0.56
C1	1.90	0.67	15.07	1.41	0.45
H ^b	1.56	0.51	3.81	1.66	0.55
C2 ^c	1.62	0.36	8.84	5.55	0.21
H	1.87	0.68	3.52	1.95	0.83
O	2.31	0.97	4.06	4.55	2.28
H ^d	2.13	0.38	2.31	2.36	0.97
H ^e	1.25	0.42	1.34	1.30	0.46
H ^e	1.22	0.38	1.42	1.16	0.42
H ^e	1.14	0.37	1.25	1.18	0.41
C ^e	1.14	0.27	2.88	1.13	0.27

^aStarting methyl group-Carbon connected to C1

^bConnected to C1

^cConnected to O

^dConnected to O

^eEnd methyl group-Carbon connected to C2

Appendix B: Free energy of solvation

Figure 7 shows an example of Hamiltonian change as the lambda changes in the slow-growth method. We are aware of the fact that by increasing the number of points we are

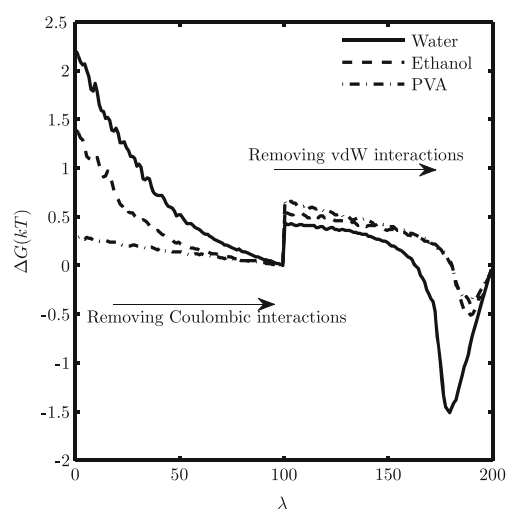


Fig. 7 A typical graph of changes in free energy during the slow-growth method. Data is related to solvation of one of the isotactic PVA oligomers

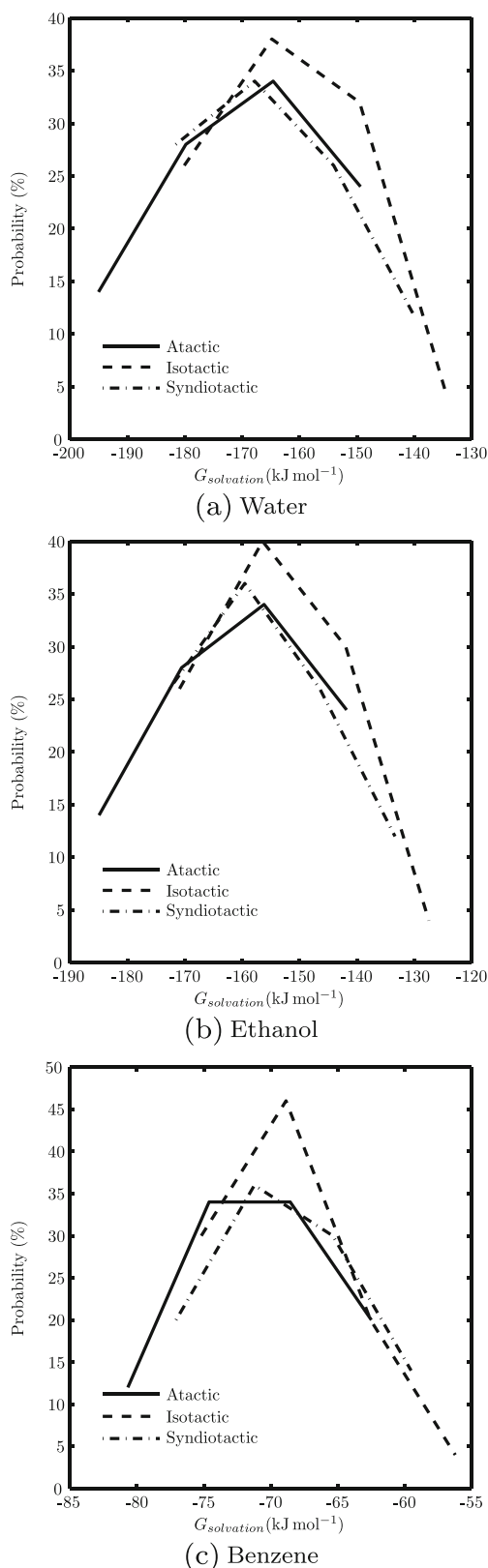


Fig. 8 Probability distribution of ab initio calculated free energy of solvation

Table 5 Average values for ab initio calculated FES

	Boltzmann weighted			Regular		
	Ata	Iso	Syn	Ata	Iso	Syn
Water	-158.3	-155.9	-148.0	-169.6	-163.0	-164.3
Ethanol	-149.5	-147.9	-138.3	-160.9	-154.8	-156.0
Benzene	-63.1	-63.9	-56.9	-70.8	-68.6	-68.8

able to obtain smoother curves (especially when vdW interactions start to vanish), but our results indicate that change in the final calculated FES would be minor.

Figure 8 shows the probability distribution for the ab initio calculated FES for oligomers of PVA in different solvents. As can be seen, these values are highly conformation dependent and are slightly different for different tacticities.

Table 5 compares the ab initio calculated FES as averaged by the Boltzmann factor with regular averaged values.

References

- Pritchard J (1970) Poly(vinyl Alcohol): basic properties and uses (polymer monographs, vol 4. Routledge
- Muller-Plathe F (1998) J Membr Sci 141:147
- Zhang QG, Liu QL, Chen Y, Wu JY, Zhu AM (2009) Chem Eng Sci 64:334
- Jang J, Lee DK (2003) Polymer 44(26):8139
- Karlsson G, Gedde U, Hedenqvist M (2004) Polymer 45(11):3893
- Patel P, Rodriguez F (1979) J Appl Polym Sci 23:2335
- Muller-Plathe F (1998) J Chem Phys 108(19):8252
- Belmares M, Blanco M, Goddard Wa, Ross RB, Caldwell G, Chou SH, Pham J, Olofson PM, Thomas C (2004) J Comput Chem 25(15):1814
- Priel S, Fermeglia M (2003) Chem Eng Commun 190:1267
- Caddeo C, Mattoni A (2013) Macromolecules 46(19):8003
- Zhang QG, Liu QL, Lin J, Chen JH, Zhu AM (2007) J Mater Chem 17(46):4889
- Durkee JB (2004) Met Finish 102(4):42
- Jawalkar SS, Adoor SG, Sairam M, Nadagouda MN, Aminabhavi TM (2005) J Phys Chem B 109(32):15611
- Patel S, Lavasanifar A, Choi P (2008) Biomacromolecules 9(11):3014
- Jawalkar SS, Raju KVS, Halligudi SB, Sairam M, Aminabhavi TM (2007) J Phys Chem B 111:2431
- Assendert HE, Windle AH (1998) Polymer 39(18):4295
- Chiessi E, Cavalieri F, Paradossi G (2007) J Phys Chem B 111(11):2820
- Hassan C, Peppas N (2000) Adv Polym Sci 153:37
- Jawalkar SS, Aminabhavi TM (2006) Polymer 47(23):8061
- Jeck S, Scharfer P, Kind M (2012) J Membrane Sci 417–418:154
- Matyjaszewski K (2002) Encycl Polym Sci Technol 8:399
- Muller-Plathe F, van Gunsteren WF (1997) Polymer 38(9):2259
- Park JS, Park JW, Ruckenstein E (2001) J Appl Polym Sci 82:1816
- Rault J, Gref R, Ping ZH, Nguyen QT, Neel J (1995) Polymer 36(8):1655

25. Rossinsky E, Tarmyshov KB, Bohm MC, Muller-Plathe F (2009) *Macromol Theory Simul* 18(9):545
26. Suchiya YT, Oshii NY, Watsubo TI (2004) *Japan J Appl Phys* 43(8A):5676
27. Tesei G, Paradossi G, Chiessi E (2012) *J Phys Chem B* 116(33):10008
28. Watanabe H, Koyama R, Hiroshi N, Nishioka A (1962) *J Polym Sci* 62(174):77
29. Takigawa T, Kashihara H, Urayama K, Masuda T (1992) *Polymer* 33(11):2334
30. Chen Nx, Zhang Jh (2010) *Chin J Polym Sci* 28(6):903
31. Jorgensen WL, Maxwell DS, Tirado-rives J (1996) *J Amer Chem Soc* 118:11225
32. Henkelman G, Arnaldsson A, Jónsson H (2006) *Comput Mater Sci* 36(3):354
33. Weiner SJ, Kollman Pa, Nguyen DT, Case Da (1986) *J Comput Chem* 7(2):230
34. Basma M, Sundara S, Calgan D, Vernali T, Woods RJ (2001) *J Comput Chem* 22(11):1125
35. Sigfridsson E, Ryde U (1998) *J Comput Chem* 19(4):377
36. Noorjahan A, Choi P (2013) *Polymer* 54(16):4212
37. Flory PJ, Leutner FS (1948) *J Polym Sci* 3(6):880
38. Accelry Inc. *Materials Studio4.0* (2005)
39. Genheden S, Soderhjelm P, Ryde U (2012) *Int J Quant Chem* 112:1768
40. Soderhjelm P, Ryde U (2008) *J Comput Chem* 30:750
41. Frisch GESMJ, Trucks GW, Schlegel HB, Robb BMMA, Cheeseman JR, Scalmani G, Barone V, Petersson HPHGA, Nakatsuji H, Caricato M, Li X, Izmaylov MHAF, Bloino J, Zheng G, Sonnenberg JL, Ehara TNM, Toyota K, Fukuda R, Hasegawa J, Ishida M, Honda JY, Kitao O, Nakai H, Vreven T, Montgomery JA, Peralta EBJE, Ogliaro F, Bearpark M, Heyd JJ, Kudin JNKN, Staroverov VN, Keith T, Kobayashi R, Raghavachari JTK, Rendell A, Burant JC, Iyengar SS, Cossi JBCM, Rega N, Millam JM, Klene M, Knox JE, Bakken RESV, Adamo C, Jaramillo J, Gomperts R, Yazyev JWO, Austin AJ, Cammi R, Pomelli C, Martin GAVRL, Morokuma K, Zakrzewski VG, Salvador ADDP, Dannenberg JJ, Dapprich S, Farkas JCO, Foresman JB, Ortiz JV, Fox DJ *Gaussian 09 Revision C.01*
42. Ruzsinszky A, Alsenoy CV (2002) *J Phys Chem A* 106:12139
43. Mulliken RS (1955) *J Chem Phys* 23(10):1833
44. Reed AE, Weinstock RB, Weinhold F (1985) *J Chem Phys* 83(2):735
45. Singh UC, Kollman Pa (1984) *J Comput Chem* 5(2):129
46. Besler BH, Merz KM, Kollman Pa (1990) *J Comput Chem* 11(4):431
47. Bader RFW (1990) *Atoms in molecules: a quantum theory*. Oxford University Press, Oxford
48. Marenich AV, Jerome SV, Cramer CJ, Truhlar DG (2012) *J Chem Theory Comput* 8(2):527
49. Ritchie JP, Bachrach SM (1987) *J Comput Chem* 8(4):499
50. Ritchie JP (1985) *J Amer Chem Soc* 107(6):1829
51. Hirshfeld FL (1977) *Theoretica Chimica Acta* 44(2):129
52. Luque FJ, López JM, Orozco M (2000) *Theor Chem Accounts: Theory, Computation, Model (Theoretica Chimica Acta)* 103(3–4):343
53. Wen M, Jiang J, Wang ZX, Wu C (2014) *Theor Chem Accounts* 133(5):1471
54. Hess B, Lutzner C, David. vdS, Lindhal E (2008) *J Chem Theory Comput* 4:435
55. Spoel DV, Lindahl E, Hess B, Groenhof G, Mark AE, Berendsen HJC (2005) *J Comput Chem* 26:1701
56. Essmann U, Perera L, Berkowitz ML, Darden T, Lee H, Pedersen LG (1995) *J Chem Phys* 103:8577
57. Lindahl E, Hess B, van der Spoel D (2001) *J Mol Model* 7:306
58. Berendsen H, van der Spoel D, van Drunen R (1995) *Comput Phys Commun* 91:43
59. Jorgensen WL, Chandrasekhar J, Madura JD, Impey RW, Klein ML (1983) *J Chem Phys* 79:926
60. Abascal JLF, Vega C (2005) *J Chem Phys* 123:234505
61. Berendsen HJC, Postma JPM, van Gunsteren J, Hermans WF (1981) In: Pullman B (ed) *Intermolecular forces*. D Reidel Publishing Company, Dordrecht, pp 331–342
62. Ryckaert JP, Ciccotti G, Berendsen HJC (1977) *J Comput Phys* 23:327
63. Berendsen HJC, Postma JPM, van Gunsteren WF, DiNola a, Haak JR (1984) *J Chem Phys* 81(8):3684
64. Klimovich PV, Mobley DL (2010) *J Comput-Aided Mol Des* 24(4):307
65. Jämbeck JPM, Lyubartsev AP (2013) *J Phys Chem Lett* 4(11):1781
66. Hockney RW, Goel SP, Eastwood JW (1974) *J Comput Phys* 14:148
67. Darden T, York D, Pedersen L (1993) *J Chem Phys* 98(12):10089
68. Abraham M, van der Spoel D, Lindahl E, Hess B (2014) *GROMACS User Manual version 5.0*
69. Shirts MR, Chodera JD (2008) *J Chem Phys* 129(12):124105
70. Jambeck JPM, Mocchi F, Lyubartsev AP, Laaksonen A (2013) *J Comput Chem* 34(3):187